Supporting Information

Wang et al. 10.1073/pnas.1205748109

SI Materials and Methods

Strains. *Caenorhabditis elegans* strains were maintained at 20 °C (1), except where noted otherwise. The WT strain is Bristol strain N2. *C. elegans* proteotoxic transgenic models include the following: CK10: *bkIs10[aex-3p::tau V337M, myo-2p::GFP]* (2); HA659: *rtIs11 [osm-10p::Htn-Q150, osm-10p::OSM-10::GFP]* (3); CL2292: *dvIs36 [pAT2 (myo-3p::GFP::degron), pRF4(rol-6(su250))]* (4); CL2006: *dvIs2 [pCL12(unc-54p::Aβ_{1-42}), pRF4 (rol-6(su1006))]* (5); AM141: *rmIs133[unc-54p::Q40::YFP]* (6); and DA2123: *adIs2122[lgg-1p::GFP::LGG-1, pRF4(rol-6(su1006))]* (7, 8).

Western Blot. Primary antibodies used in the study were anti-ubiquitin (sc-8017; Santa Cruz Biotechnology), anti-GFP (14606200; Roche), and anti-actin (ab1801; Abcam). Phosphorylation-independent tau antibody (clone TAU-2, T-5530; Sigma). Antibodies for phosphorylated tau included pSer396 (T-7319; Sigma), pSer409 (T-7694; Sigma), pSer214 (T-7819; Sigma), and AT8 for pSer202/pThr205 (MN1020; Thermo Scientific).

SYBR Green Real-Time PCR. The transcript level of different transgenes in WT and β-*N*-acetyl-D-glucosamine (O-GlcNAc) cycling mutants were measured with quantitative RT-PCR (qPCR). The primers were chosen to amplify specifically the mRNA transcript from the transgenes encoding the N terminus of human huntingtin protein in Htn-Q150, YFP in Q40-YFP (pEYFP-N1 as template; Clontech), amyloid β_{1-42} peptide in CL2006 (9), or different splicing isoforms of *daf-16*. Total RNA was isolated from synchronized animals of the developmental stages closest to the time point when the proteotoxic phenotypes were scored, i.e., fourth larval stage for tau (V337M), 1-d-old adults for Htn-Q150, fourth larval stage for Q40-YFP, and 1-d-old adults at 25 °C for Aβ_{1-42} animals. SYBR green real-time PCR was performed with the cDNA synthesized from isolated total RNA. The actin-encoding gene *act-1* was used as an internal control. The relative level of the transcript of different transgenes in O-GlcNAc cycling mutants was calculated by comparing to the control strain that expressed the same transgene in an otherwise WT background.

The gene expression of DAF-16 targets, and several transthyretin-like genes, was examined with customized *C. elegans* StellARray qPCR Arrays (Lonza). Total RNA was isolated and treated with DNase as described earlier. cDNA was synthesized with qScript cDNA SuperMix (Quanta Biosciences), mixed with RT^2 SYBR Green qPCR Master Mix (Qiagen), and loaded onto the qPCR arrays. The real-time PCR results were analyzed with Global Pattern Recognition (Lonza).

1. Brenner S (1974) The genetics of Caenorhabditis elegans. *Genetics* 77:71–94.
2. Kraemer BC, et al. (2003) Neurodegeneration and defective neurotransmission in a Caenorhabditis elegans model of tauopathy. *Proc Natl Acad Sci USA* 100:9980–9985.
3. Faber PW, Alter JR, MacDonald ME, Hart AC (1999) Polyglutamine-mediated dysfunction and apoptotic death of a Caenorhabditis elegans sensory neuron. *Proc Natl Acad Sci USA* 96:179–184.
4. Link CD, et al. (2006) Conversion of green fluorescent protein into a toxic, aggregation-prone protein by C-terminal addition of a short peptide. *J Biol Chem* 281:1808–1816.
5. Link CD (1995) Expression of human beta-amyloid peptide in transgenic Caenorhabditis elegans. *Proc Natl Acad Sci USA* 92:9368–9372.
6. Morley JF, Brignull HR, Weyers JJ, Morimoto RI (2002) The threshold for polyglutamine-expansion protein aggregation and cellular toxicity is dynamic and influenced by aging in Caenorhabditis elegans. *Proc Natl Acad Sci USA* 99:10417–10422.
7. Kang C, You YJ, Avery L (2007) Dual roles of autophagy in the survival of Caenorhabditis elegans during starvation. *Genes Dev* 21:2161–2171.
8. Meléndez A, et al. (2003) Autophagy genes are essential for dauer development and life-span extension in C. elegans. *Science* 301:1387–1391.
9. Cohen E, Bieschke J, Perciavalle RM, Kelly JW, Dillin A (2006) Opposing activities protect against age-onset proteotoxicity. *Science* 313:1604–1610.

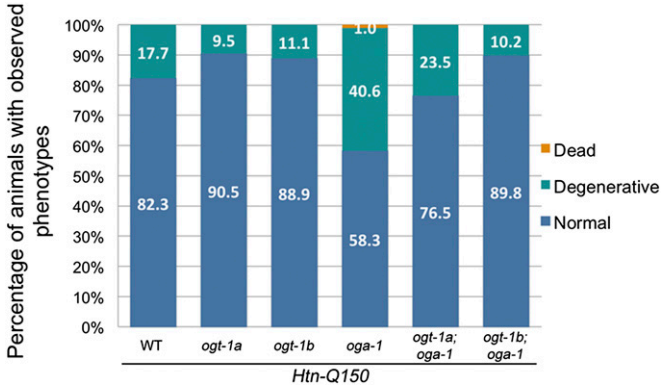

Fig. S1. The percentage of normal, degenerative, and dead ASH neurons of the total ASH neurons scored in 3-d-old adults from WT and O-GlcNAc cycling single and double mutants. *ogt-1a* represents *ogt-1*(*ok430*), *ogt-1b* represents *ogt-1*(*ok1474*).

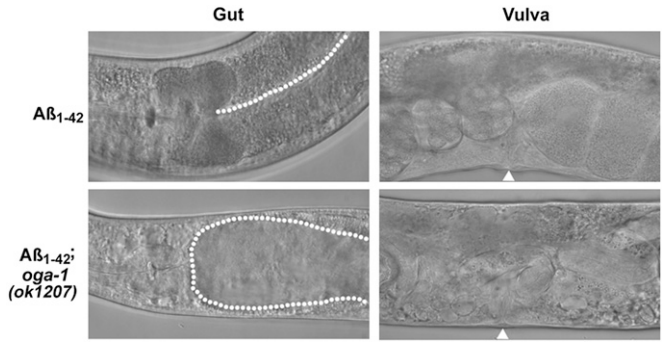

Fig. S2. The *oga-1* mutation enhanced the $A\beta_{1-42}$ toxicity in enteric muscles and sex muscles, causing constipated and egg-laying defective phenotypes, indicated by expanded intestinal lumen (*Left*, outlined by white dashed line) and retained hatched larvae in uterus (*Right*), respectively. White arrowhead indicates vulva opening.

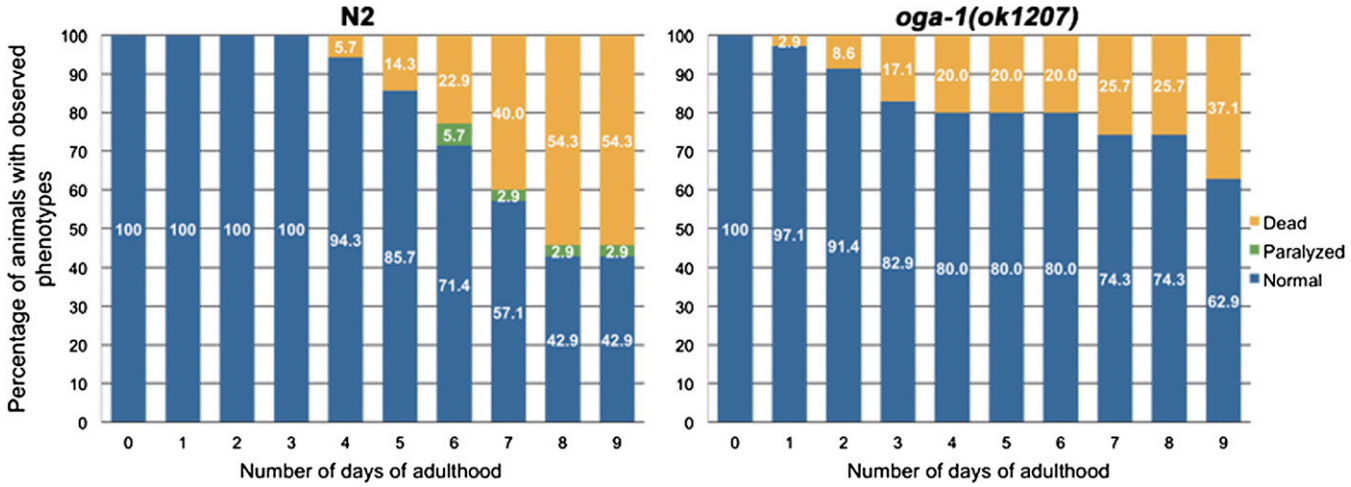

Fig. S3. N2 WT (*Left*) and *oga-1*(*ok1207*) mutant (*Right*) did not show obviously paralyzing phenotype under the same condition used to score $A\beta_{1-42}$ and GFP-degron toxicity to muscle cells.

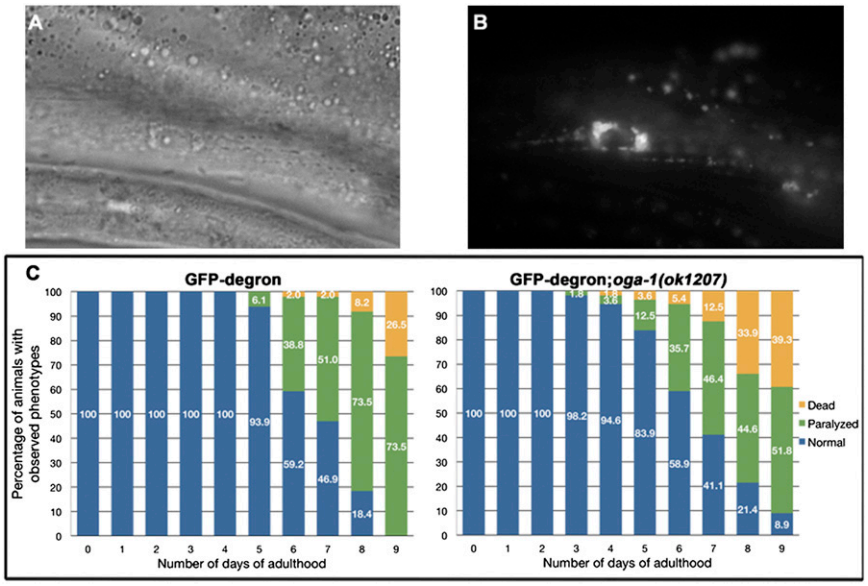

Fig. S4. (*A* and *B*) DIC and fluorescent images of GFP-degron show perinuclear aggregates in body wall muscle. (*C*) The *oga-1*(*ok1207*) mutation did not alter the proteotoxic phenotype of GFP-degron.

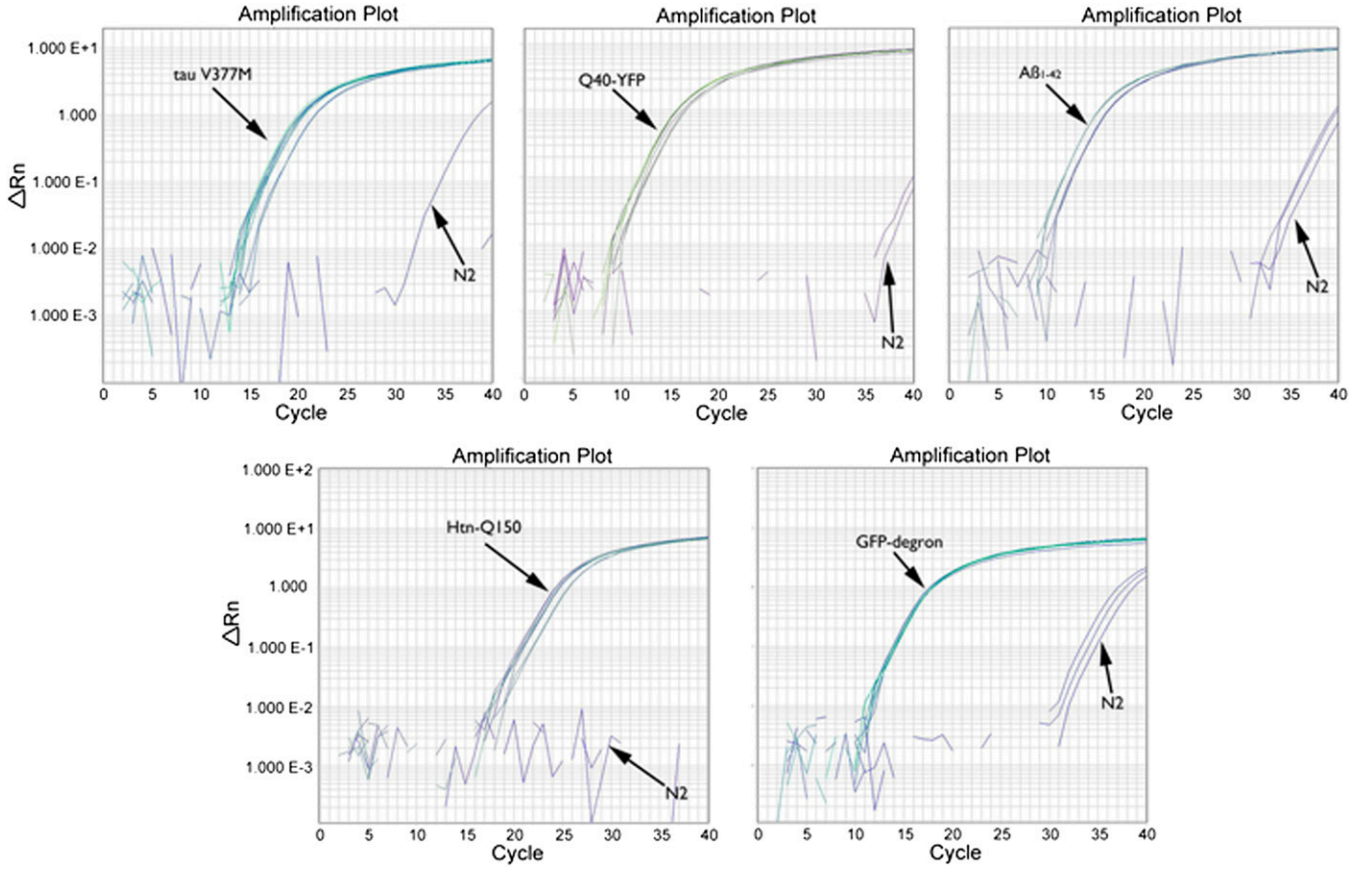

Fig. S5. Quantitative RT-PCR of indicated transgenes in different neurodegenerative models and N2 worms. The expression of the transgene mRNA in WT, *ogt-1*, or *oga-1* null mutant background was identical or showed minor differences. However, in N2 worms, only nonspecific signal was detected around 35 cycles.

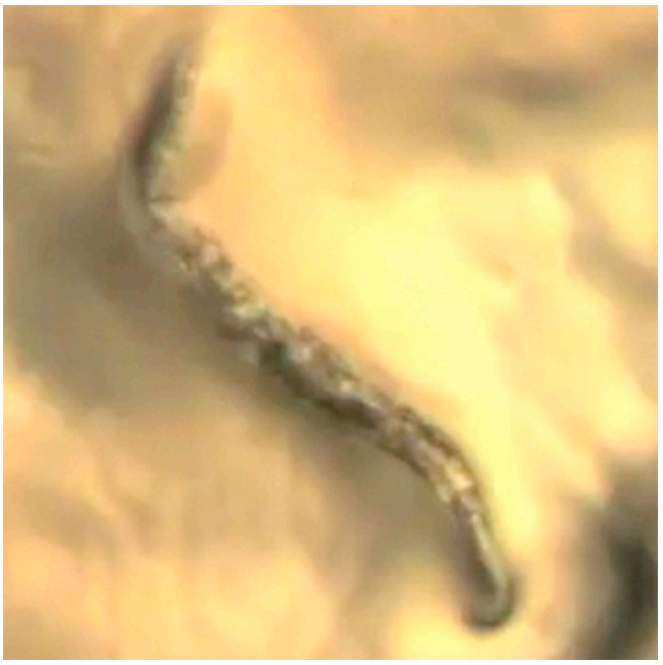

Movie S1. An $A\beta_{1-42}$ animal paralyzed on nematode growth medium plate, with a "halo" formed around its head (as a result of limited body movement and feeding on the bacterial lawn).

Movie S1

Movie S2. A WT N2 animal shows active thrashing movement in liquid.

Movie S2

Movie S3. A tau V337M transgenic animal shows defective thrashing movement in liquid, with a kinked tail unable to move coordinately with the head.

Movie S3

Movie S4. Defective thrashing movement of a tau V337M animal is rescued in the *ogt-1*(*ok430*) mutant background.

Movie S4

Movie S5. The *oga-1*(*ok1207*) mutation did not alter the defective thrashing movement of a tau V337M animal.

Movie S5

Dataset S1. Genes with significant changes in expression in different proteotoxicity models in the O-GlcNAc cycling mutant backgrounds

Dataset S1

Dataset S2. Raw expression data of genes examined with high-throughput qPCR in different proteotoxicity models in the O-GlcNAc cycling mutant backgrounds

Dataset S2